High-energy structures in the gamma-ray spectra of the fusion-fission reaction $^{238}U + {}^{9}Be$

MICHAŁ CIEMAŁA

IFJ PAN, KRAKÓW

~~08/05/2025~~ 05/06/2025

Prompt fission gamma-rays (PFGS)

Fission-related observables, such as fragment and prompt neutron characteristics, have been extensively studied both experimentally and theoretically over recent decades. More recently, there has been growing interest in measuring prompt gamma-rays and their correlations with other observables.

Experimental data on the high-energy part of the prompt fission gamma spectrum (PFGS) remains limited, with the earliest studies dating back to the 1970s.

High energy structures in the gamma-ray spectrum were observed during this measurments, however up to this day with no isotopic identification of the emiter(s) nor its origin.

Prompt fission gamma-rays (PFGS)

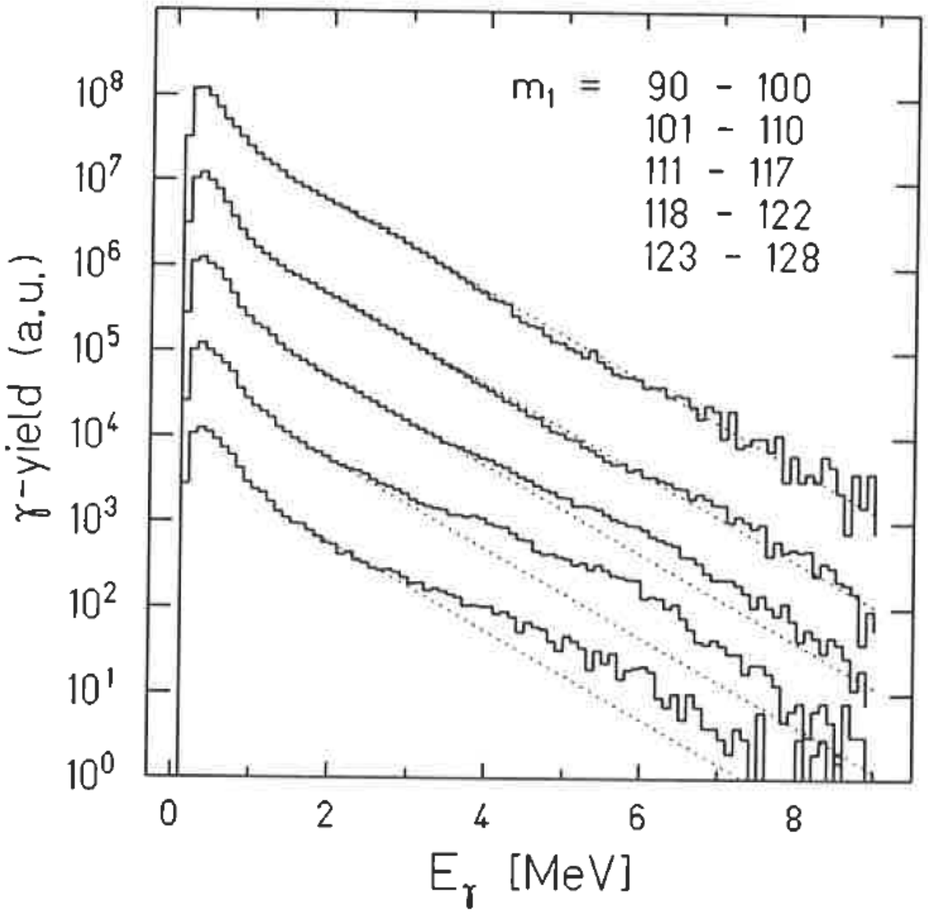

Non-statistical high energy gamma's
"These high-energy tails exhibit a marked dependence on fragment mass."

^{252}Cf fission revisited - new insights into the fission process

P. Glässel, et al., Nuclear Physics A, 502, 1989, 315.

Detectors: NaI, Crystall Ball

Prompt fission gamma-rays (PFGS)

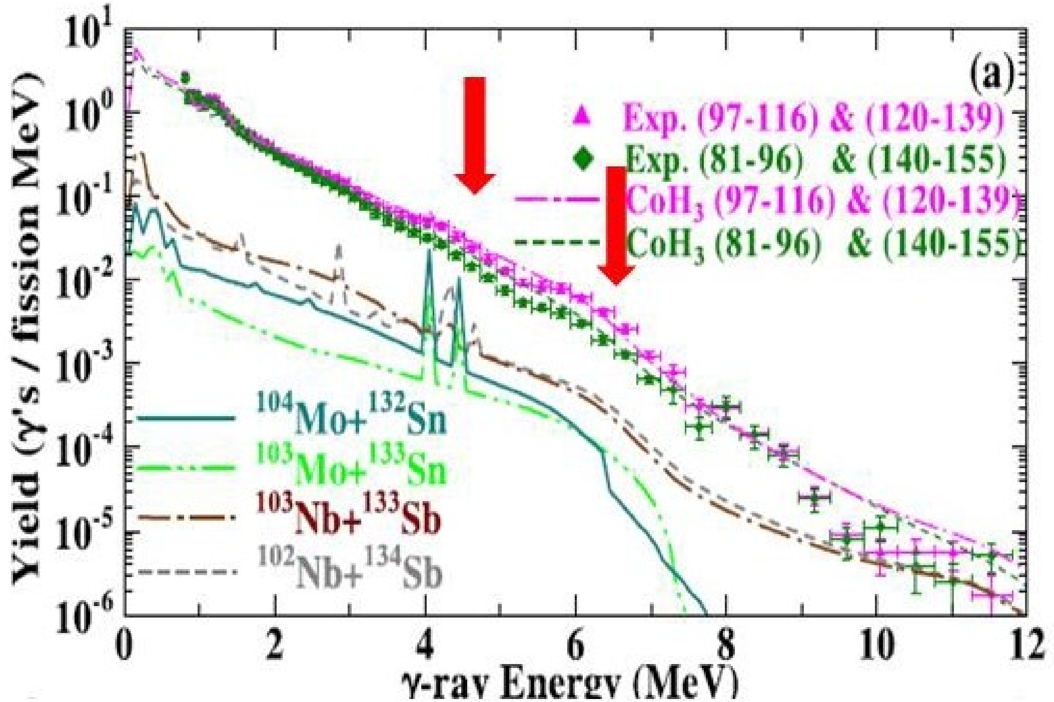

Makii et al., conclude that the bump at around 4MeV is created by the transitions between the discrete levels in the fragments around ^{132}Sn, and the bump at around 6MeV mostly comes from the complementary light fragments.

Effects of the nuclear structure of fission fragments on the high-energy prompt fission γ-ray spectrum in $^{235}U(n,f)$

H. Makii, et al., Phys. Rev. C 100 (2019) 044610.

Detectors: $LaBr_3$

Prompt fission gamma-rays (PFGS)

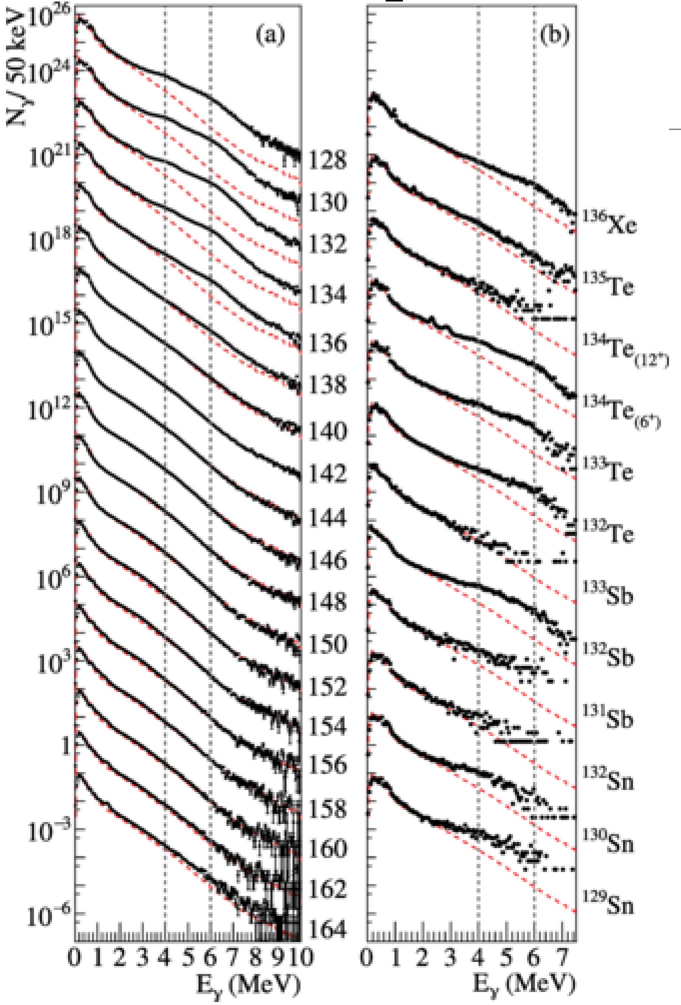

"Enhanced production of prompt γ rays peaked at 4 and 6 MeV in the mass region of fission fragments around 132Sn is a known phenomenon for 30 years. Various contradictory interpretations of their origin can be found in the literature: either discrete or statistical γ rays originating from the light or heavy fragment."

Conclusion:

"From the study of the photon emission probability we interpret these structures as arising from the competition between the “strength-driven” decay of the heavy fragments and the “density-driven” decay of the light fragments."

Detectors: NaI

Origin of the high-energy structures in the prompt-fission γ-ray spectrum of 252Cf

A. Francheteau, et al., Phys. Rev. C 111, 034608, march 2025

VAMOS + PARIS& EXOGAM @ GANIL

Ch. Schmitt, M. Ciemała, et al.

Fusion-fission reaction in inverse kinematics

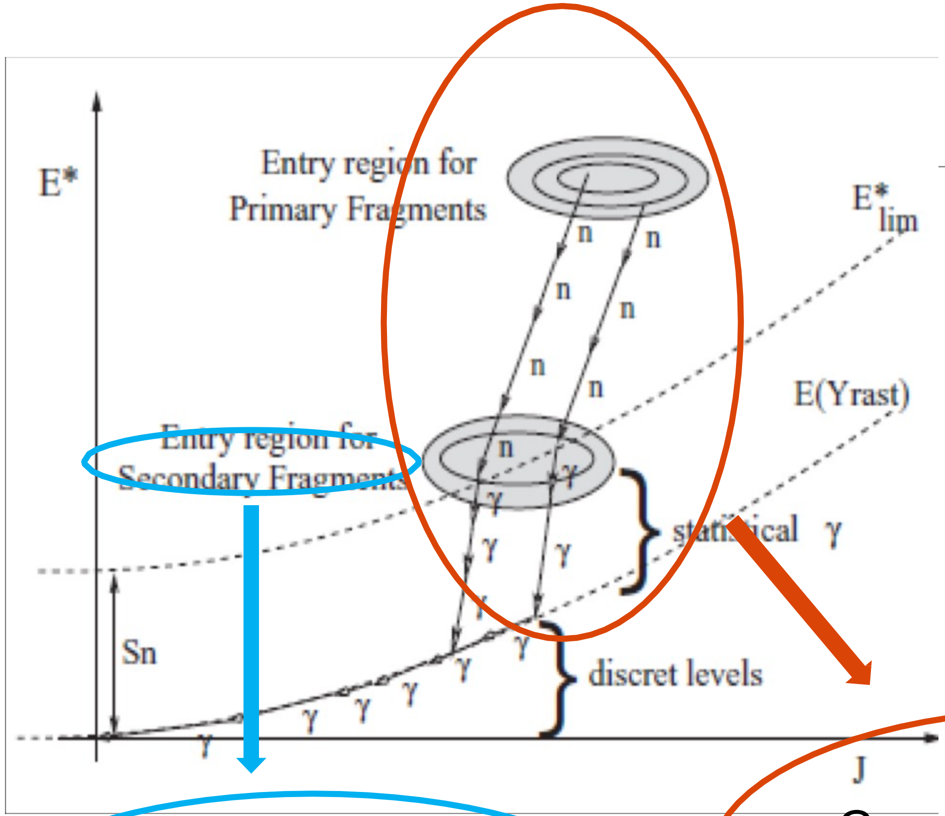

Inverse kinematics provides the capability of fission fragments nuclear charge identification

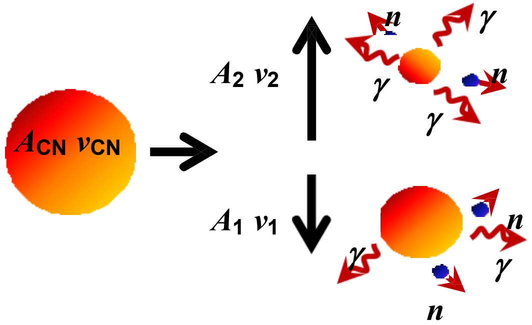

magnetic spectrometer: angle, velocity and $(A,Z)_{FF}$ identification

+

Gamma calorimeter: M_γ and E_γ spectrum up ~30 MeV

+

GANIL heavy beams

=

Unique Tool

GANIL E826 : VAMOS+PARIS&EXOGAM experiment performed 2022

Fusion-fission in inverse kinematics

$^{238}U + {}^{9}Be \rightarrow {}^{247}Cm^{*}$ **($E^{*}\sim$ 43MeV)**

(5.88MeV/u) (500µg/cm2)

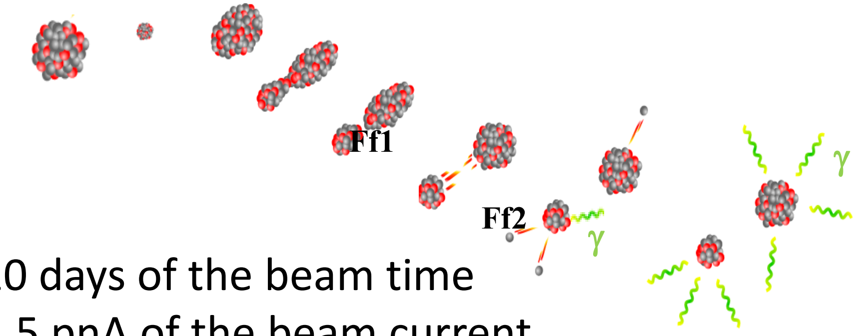

10 days of the beam time

1.5 pnA of the beam current

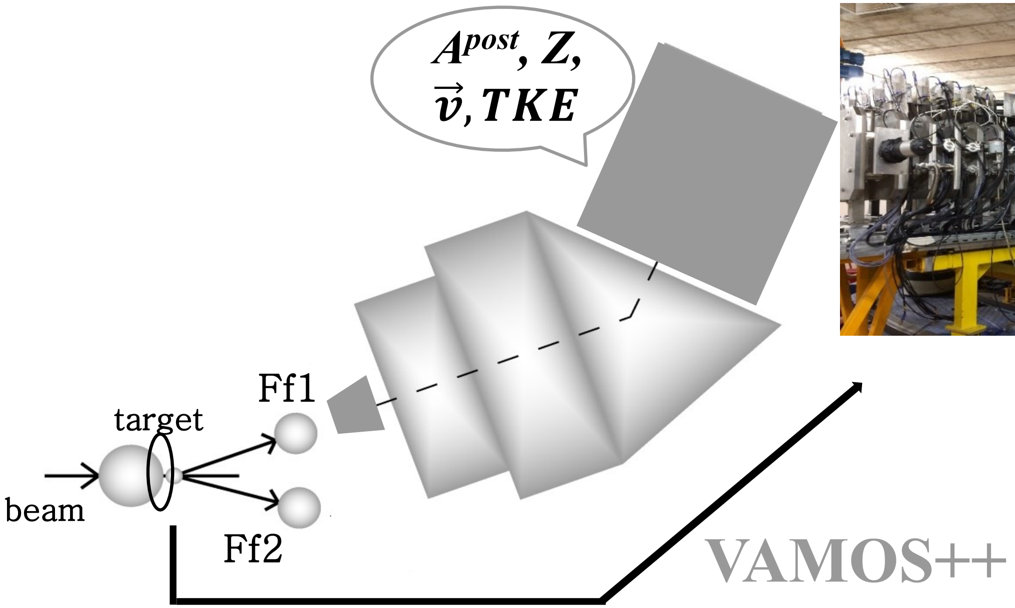

ϑ=21°, Bρ=1.1Tm

event by event

- ✓ **Ff's uniquely resolved / characterized in (A, Z, $\vec{v}$)**
- ✓ **PFGS and properties (E_{γ}, E_{γ}^{sum}, M_{γ})**
- ✓ **Neutrons (E_{n} , M_{n})**

PFGS

E_{γ}, E_{γ}^{sum}, M_{γ}, M_{n}

PARIS

Exogam

PARIS array properties

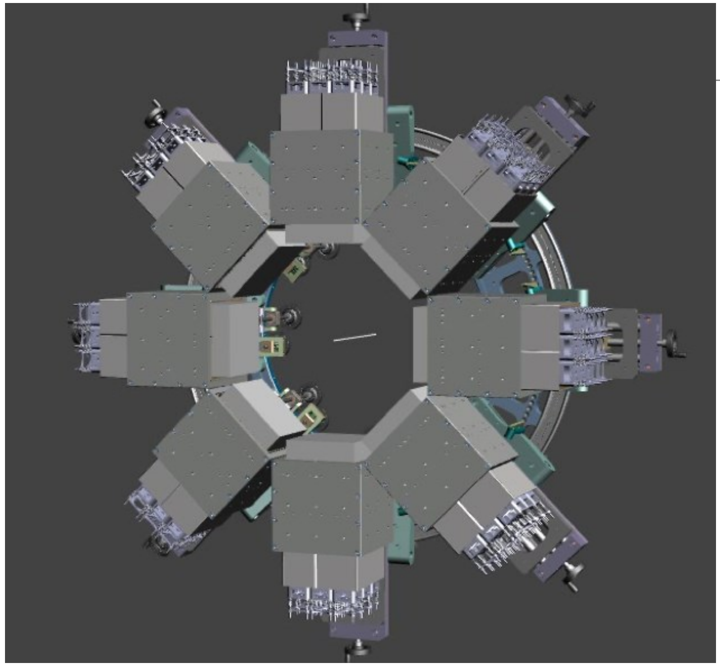

Good energy resolution for low and high energy γ-rays

- 35 keV @ 1.332 MeV

Excellent Time resolution (below ~ 1 ns)

Measurement of gamma multiplicity from frontal $LaBr_3$ or $CeBr_3$

Large efficiency for high energy γ-rays (~ 5% at 10 MeV for 8 clusters)

72 phoswiches in 8 clusters

72 LaBr3:Ce or CeBre 2”x2” crystals in 8 clusters

~ 28 liters of NaI in 8 clusters

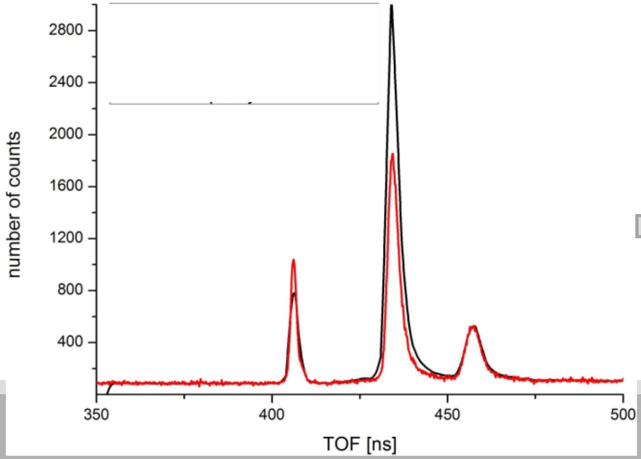

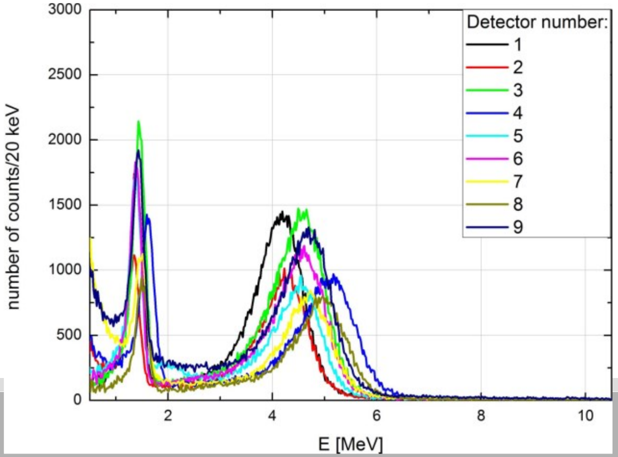

Previous use of PARIS in PFGS/PFNS:

E. Kozulin et al., Eur. Phys. J A 56 (2020) 6

E. Vardaci et al., Phys. Rev. C 101 (2020) 064612

L. Qi et al., Eur. Phys. J A 56 (2020) 98

Example of neutron measured by PARIS via ToF

Examples of PARIS spectra

1 phoswich

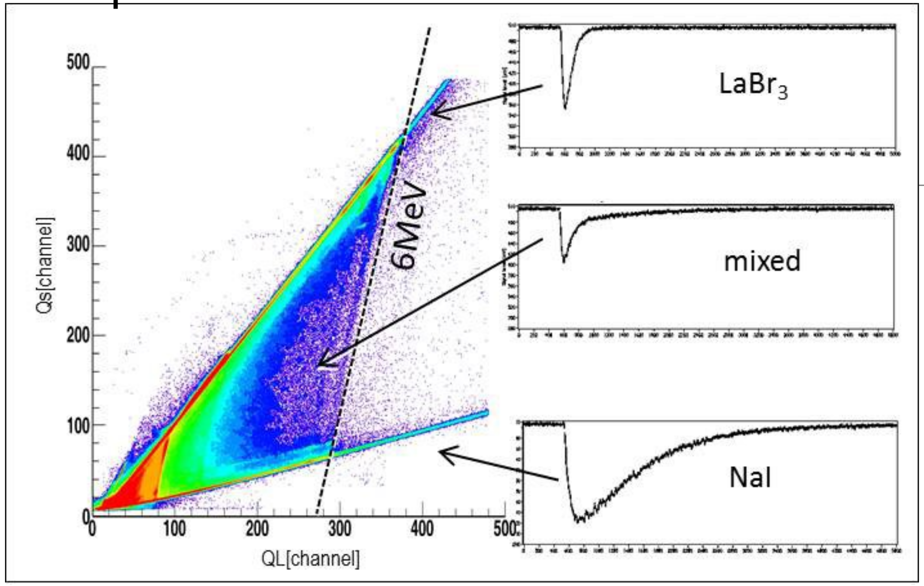

1 cluster

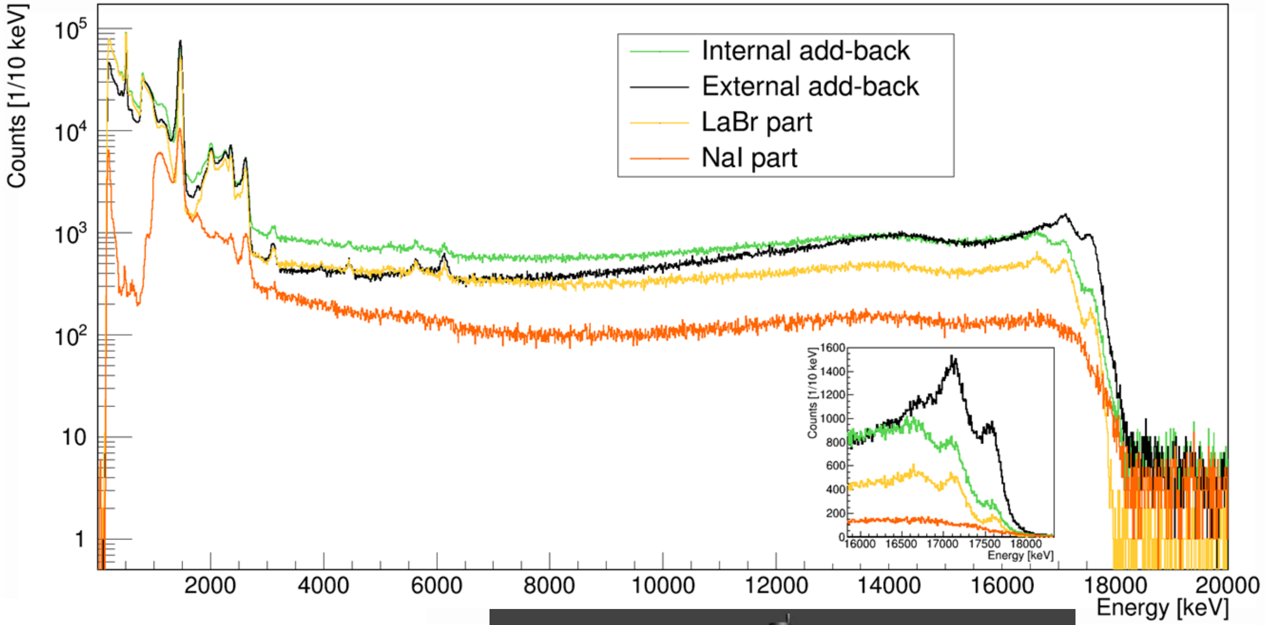

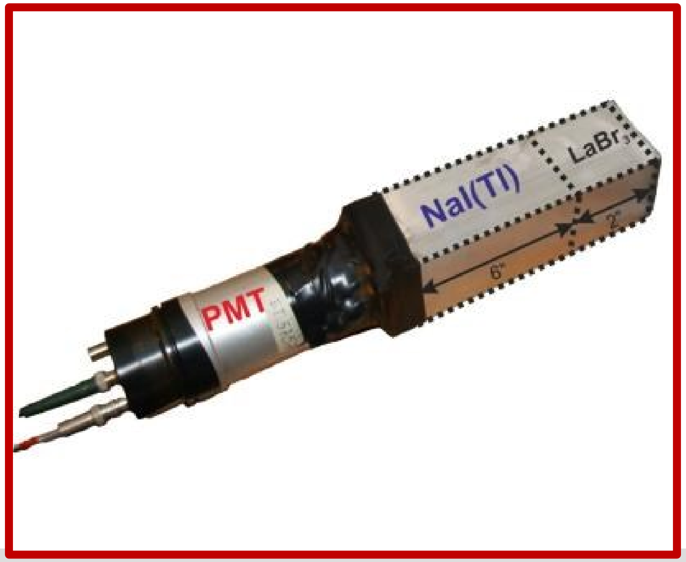

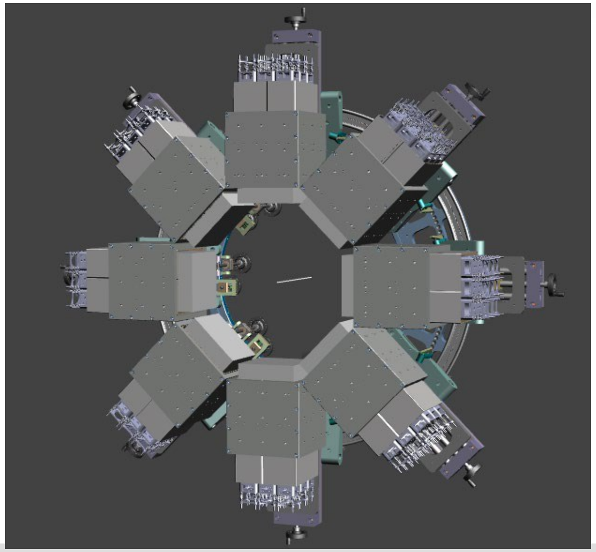

A,Z, VAMOS spectrometer identification

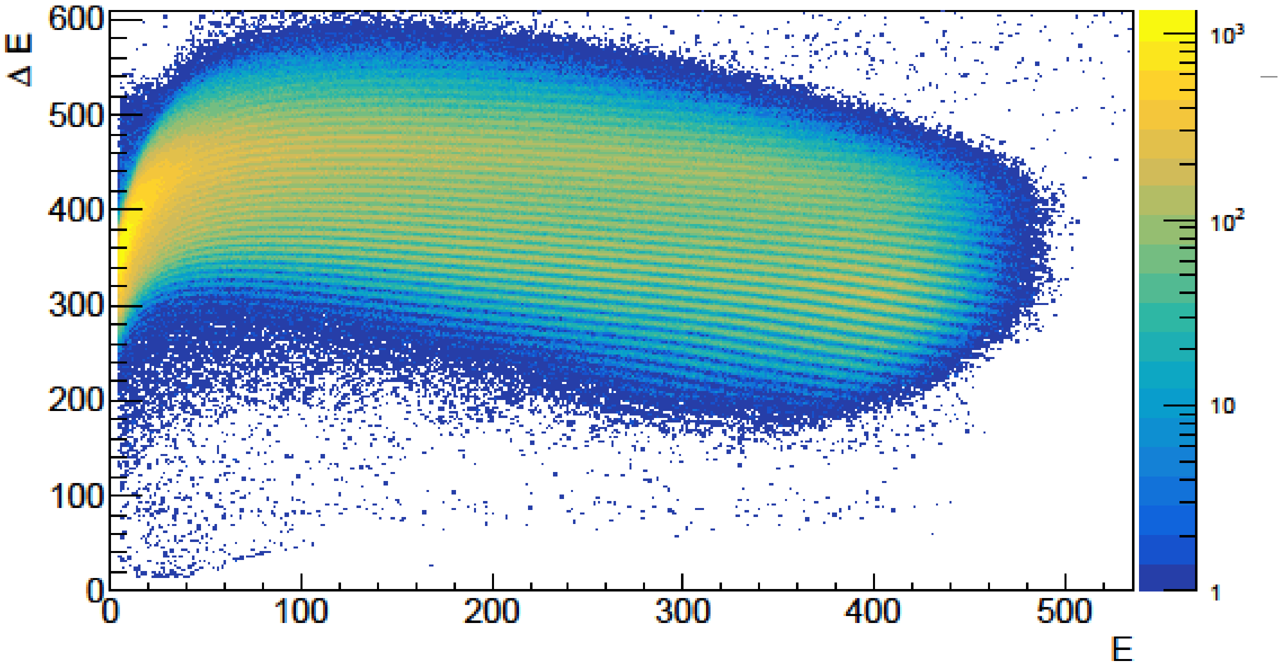

Correlation between the energy loss and total energy deposit in the VAMOS++ ionization chamber - Z identification

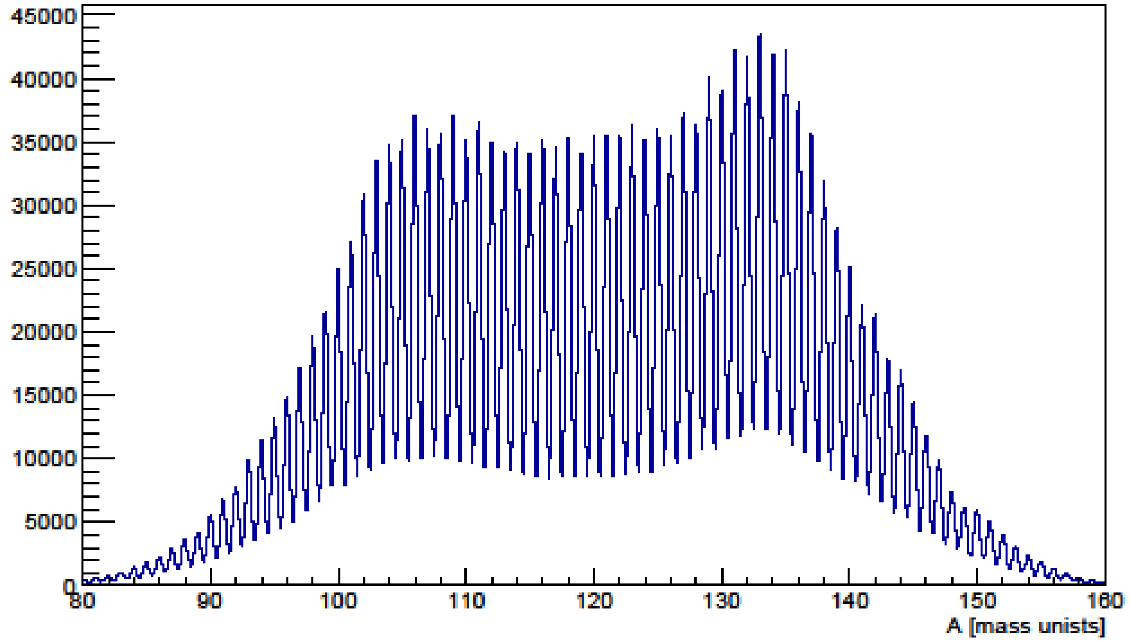

Detected post-neutron mass spectrum

The resolution achieved in the present experiment was **1/200** in mass and **1/68** in charge.

Promp gamma-ray: time measurement

Shape of the background in high energy (6-10 MeV) gamma-ray region

Perfect **time resolution (around 0.6 ns)** of PARIS is crucial for the high Energy region of the gamma-ray spectrum

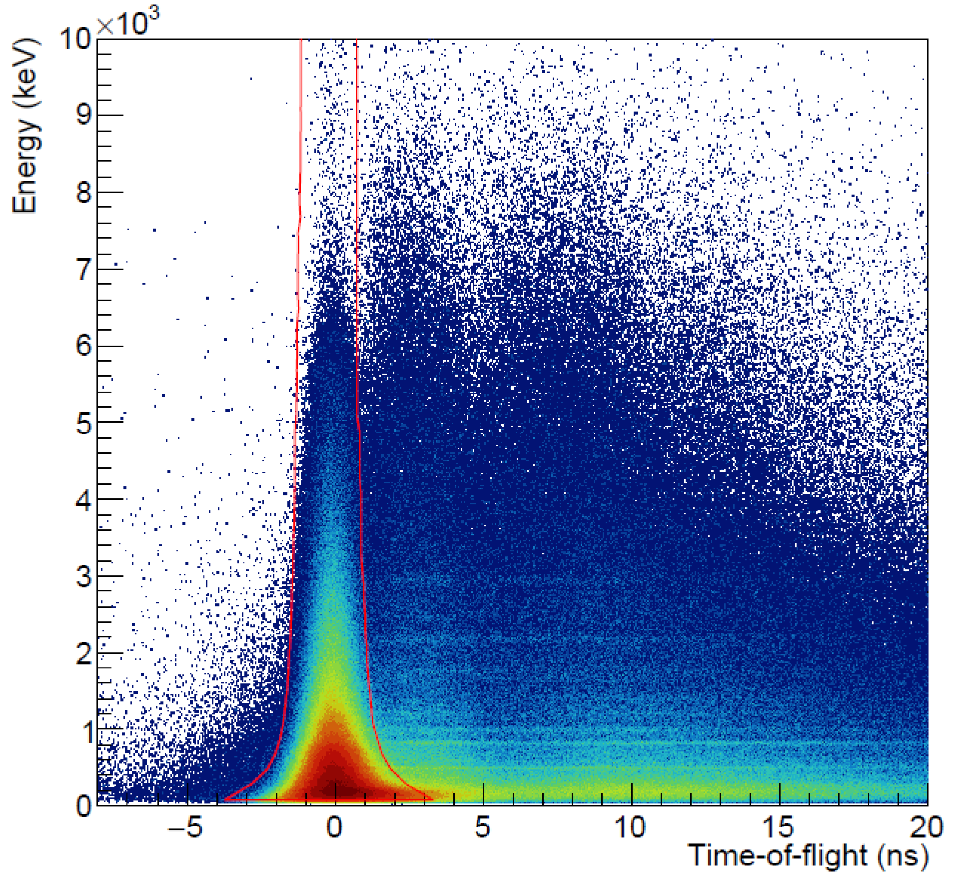

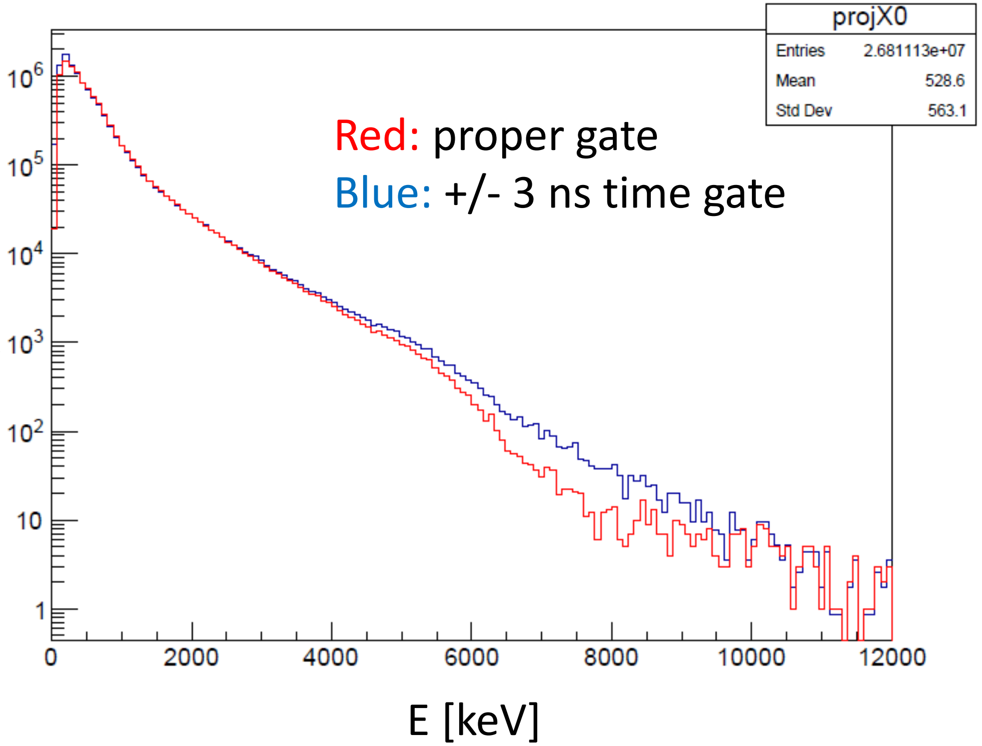

PARIS add-back

Summing of Energy deposits inside PARIS cluster

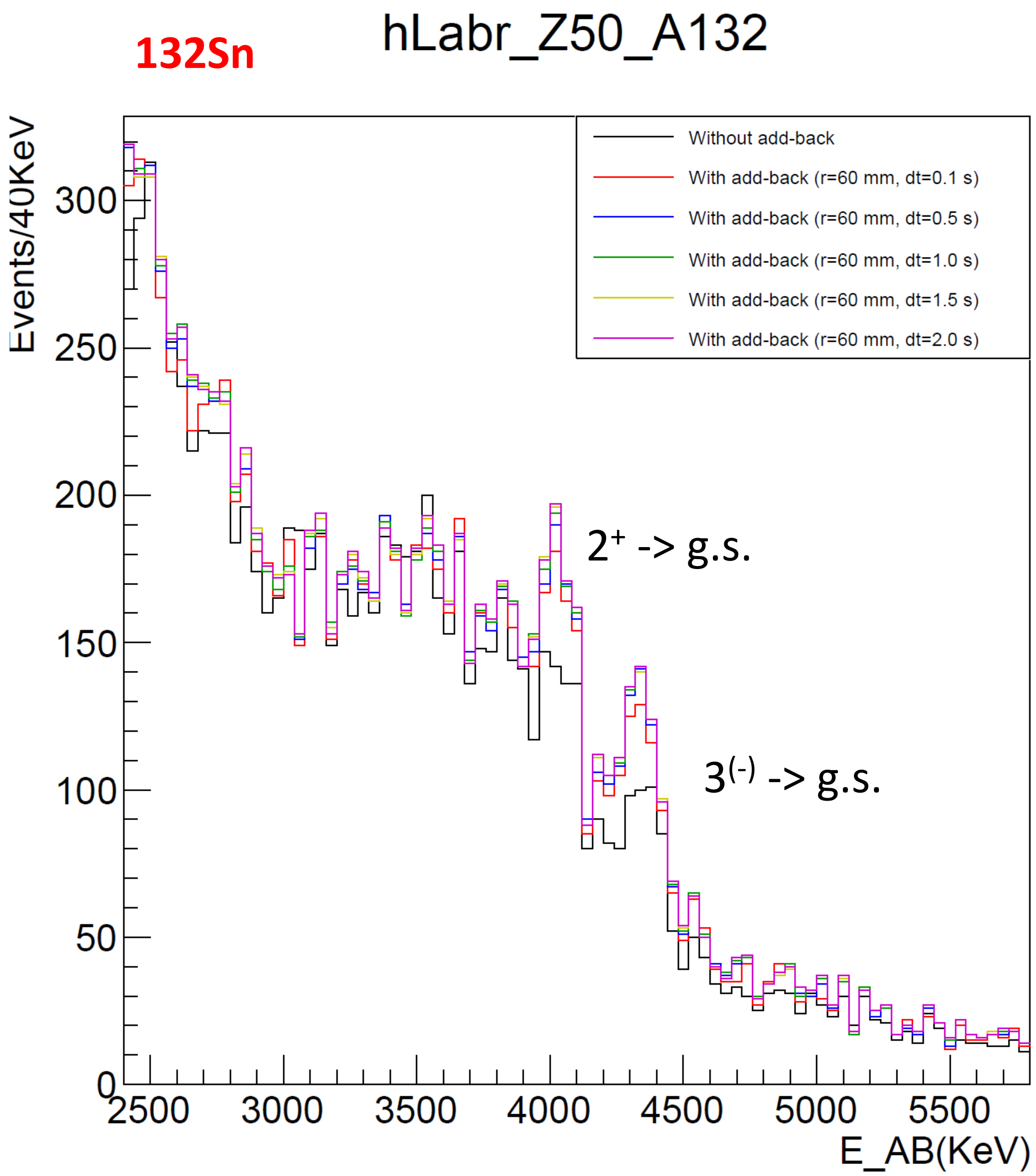

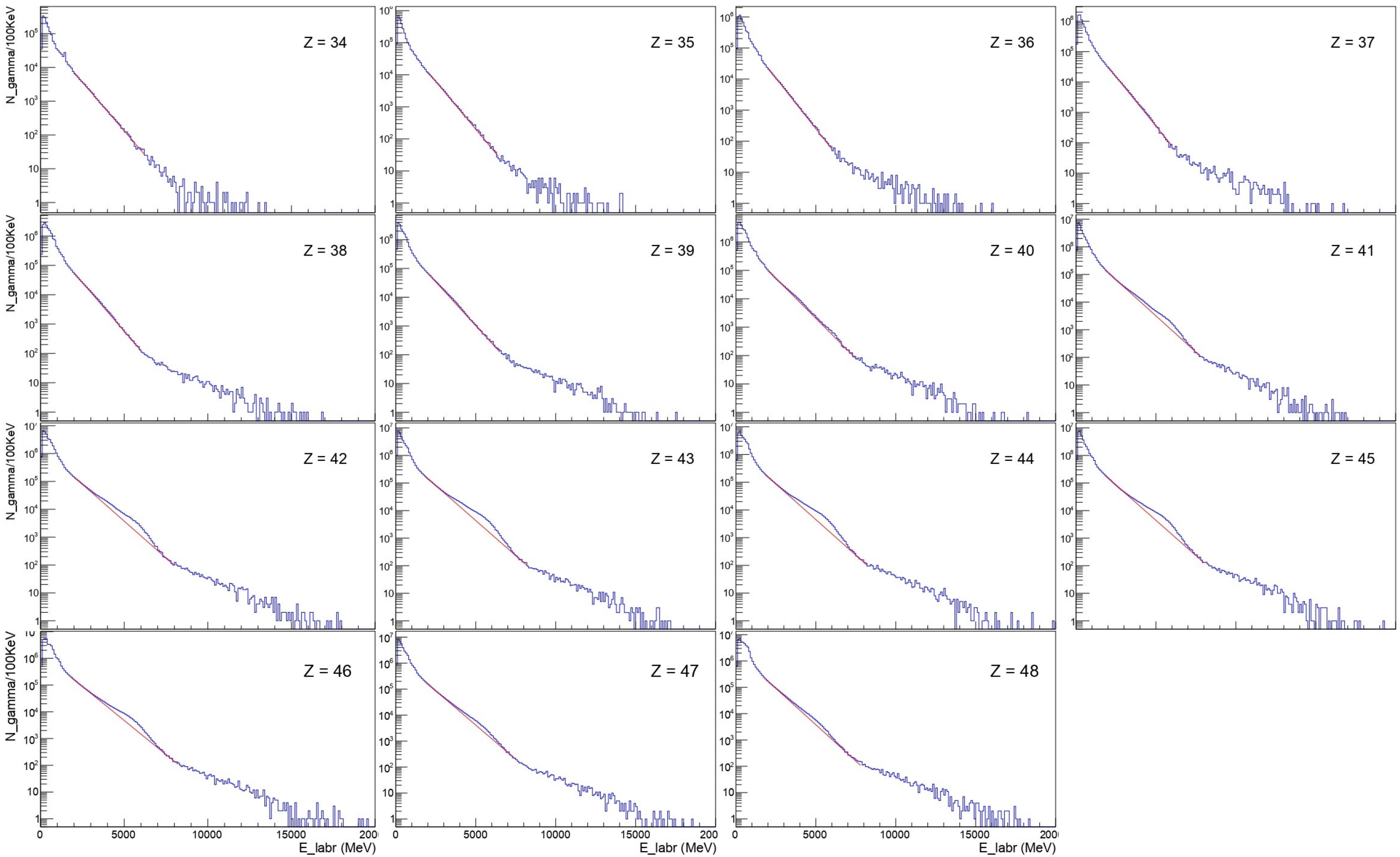

Z gated γ properties - PFGS

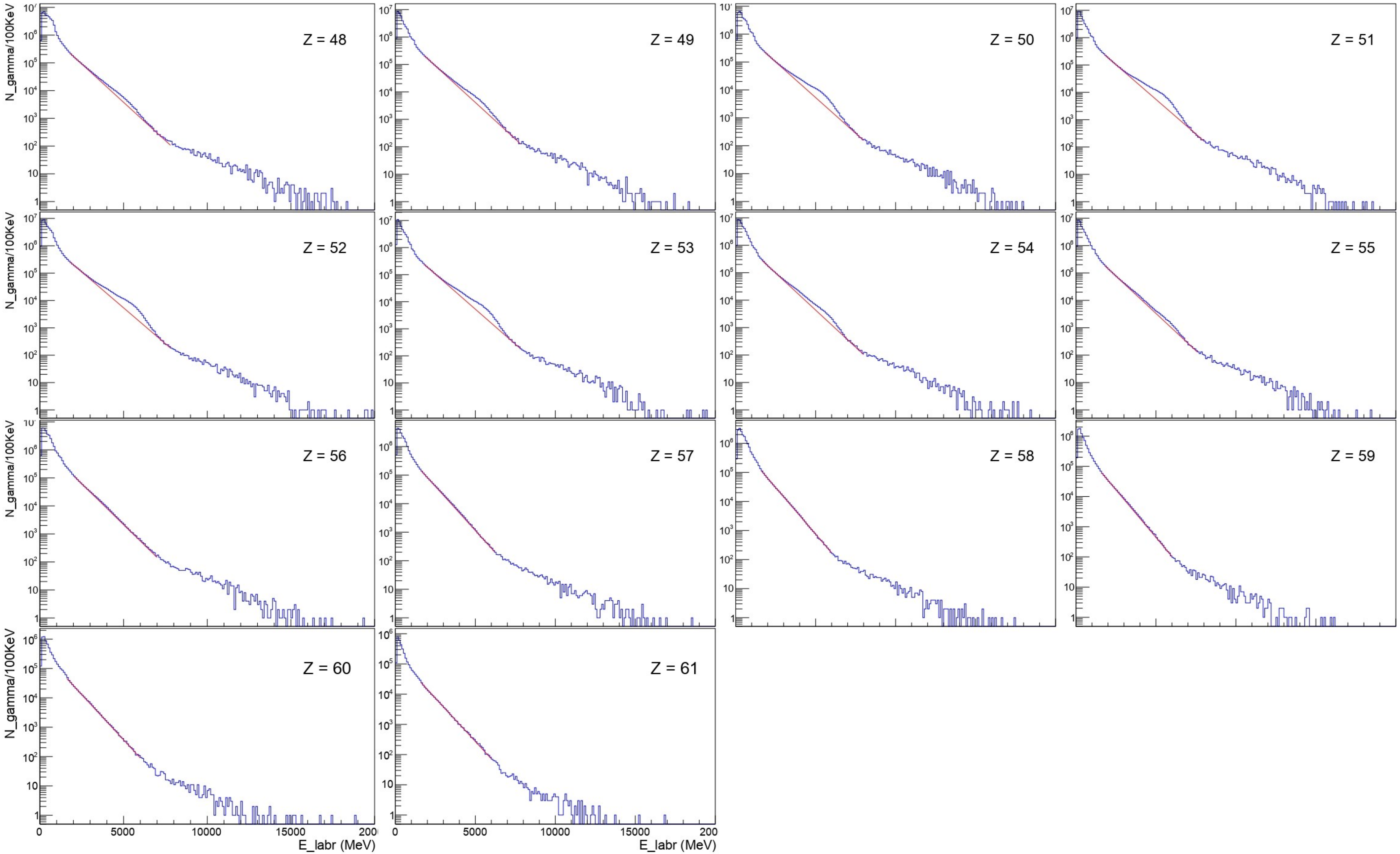

Z gated γ properties - PFGS

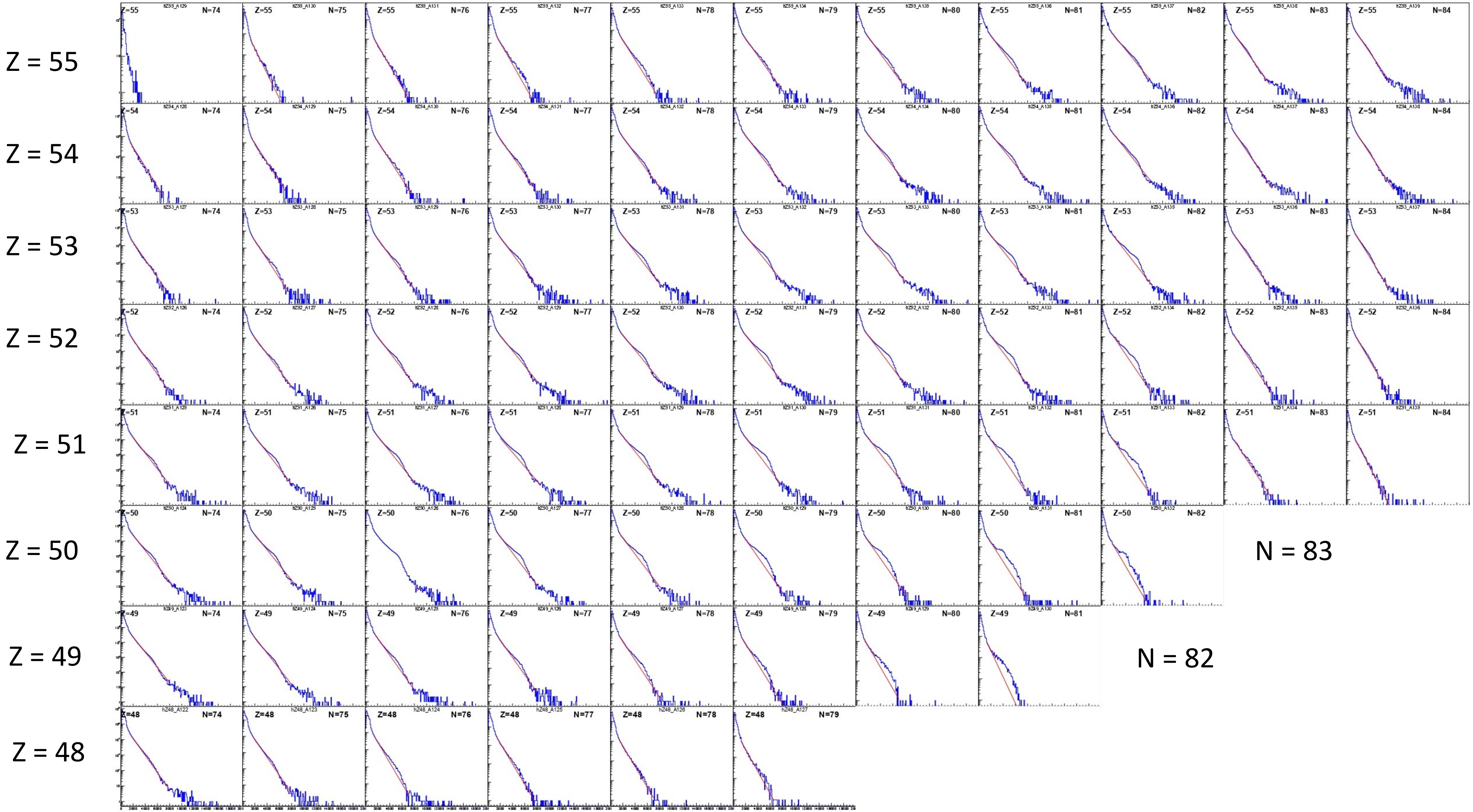

N,*Z* gated γ properties - PFGS

N,Z gated γ properties – PFGS, origin, Doppler

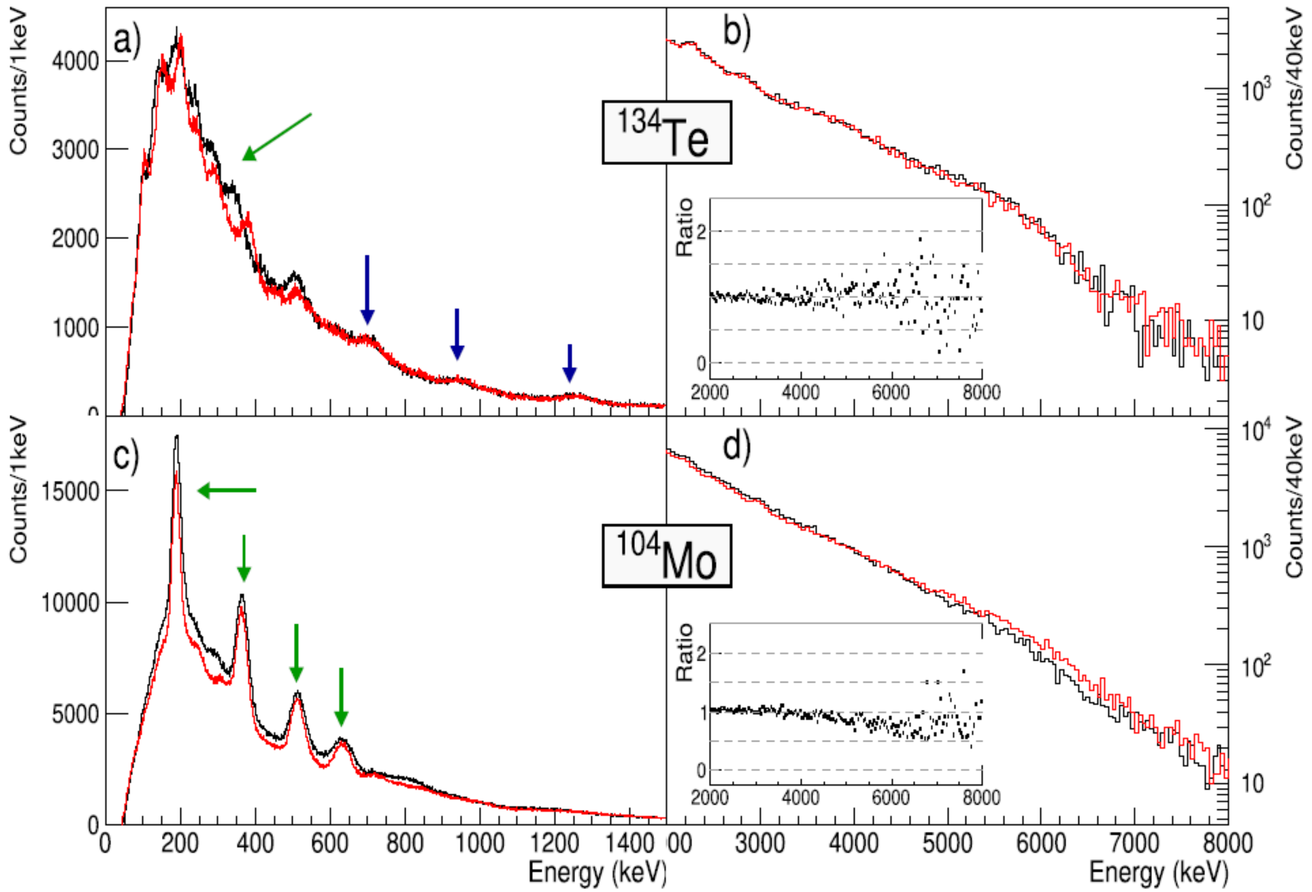

a) and b): PFGS for ^{134}Te in VAMOS++, in the low and higher E range.

Red and black refer to the spectrum defined as forward and backward, respectively. Blue arrows show transitions from ^{134}Te, while green points the region characteristic of the light partners.

c) and d): Same for ^{104}Mo in VAMOS++. Green arrows show transitions from ^{104}Mo.

Conclusion: Emission from heavy partner

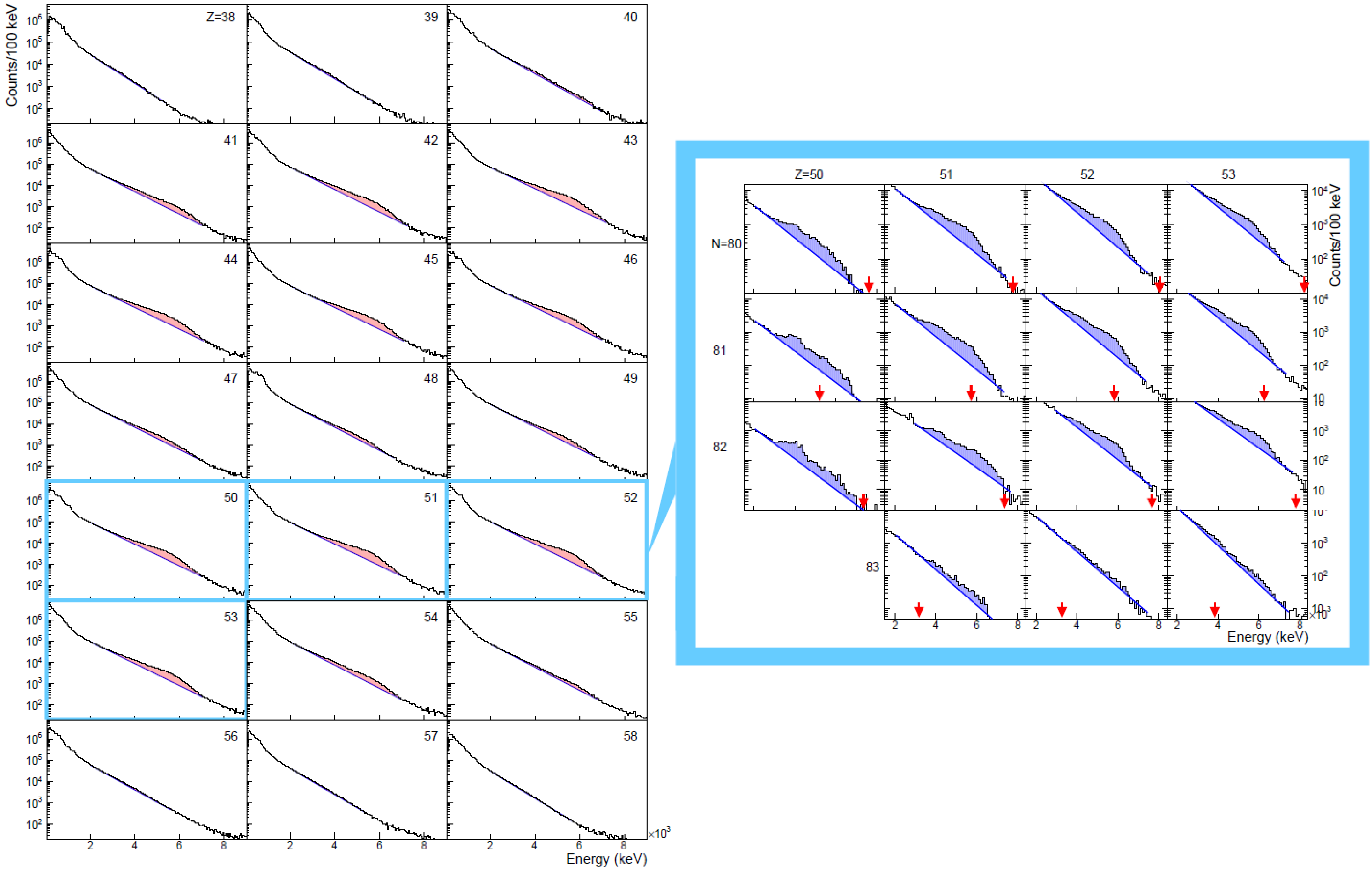

N,*Z* gated γ properties - PFGS

FIFRELIN code calculations

FIFRELIN is one of the best models for describing the de-excitation of the fragments produced in fission. It computes neutron and gamma-ray within the Hauser-Feschbach formalism with empirical inputs wherever available, and empirically-determined parameters otherwise. It includes microscopic nuclear level densities (D1M) and photon strength functions for electric and magnetic dipole transitions (D1M+QRPA)

Calculations were done for ^{247}Cm (including multi-chance fission), ^{240}Pu, and ^{238}U, which weight was estimated based on experimental observations.

O. Litaize, et al., Eur. Phys. J. A 51 (2015) 77.

FIFRELIN code calculations, entry point

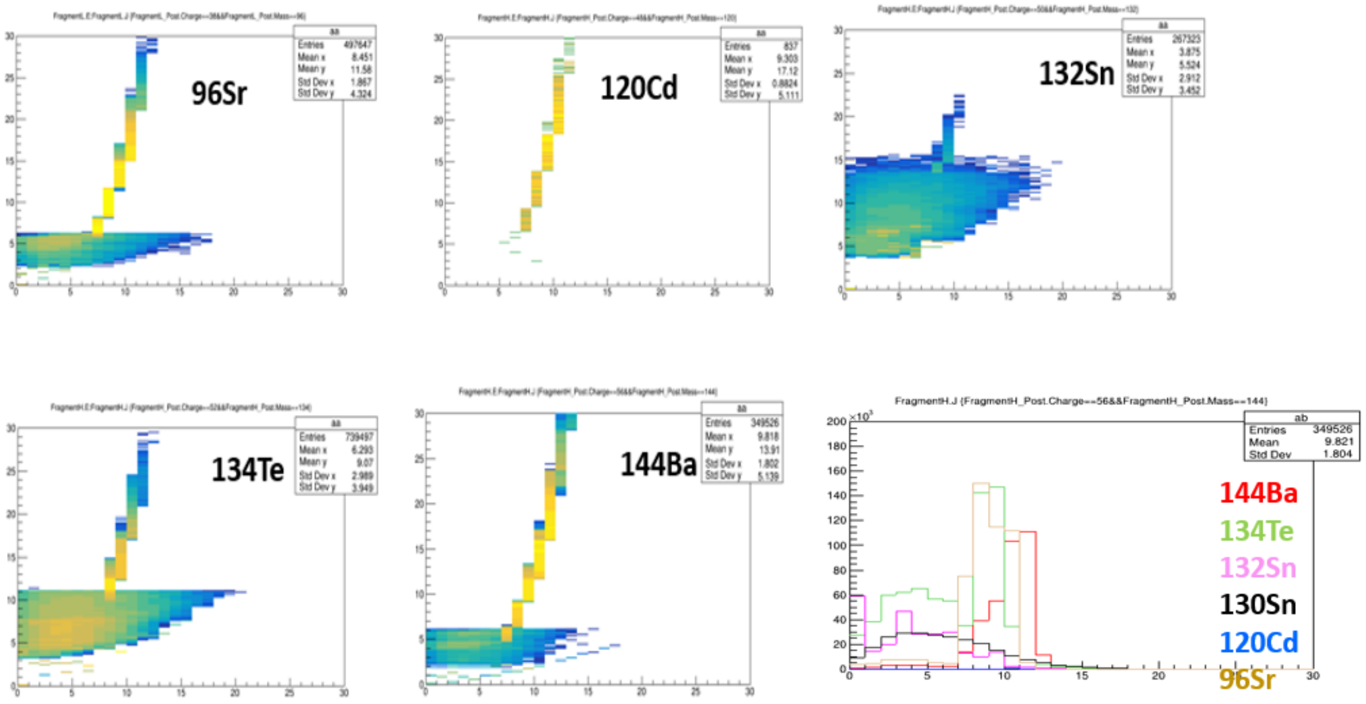

CALC

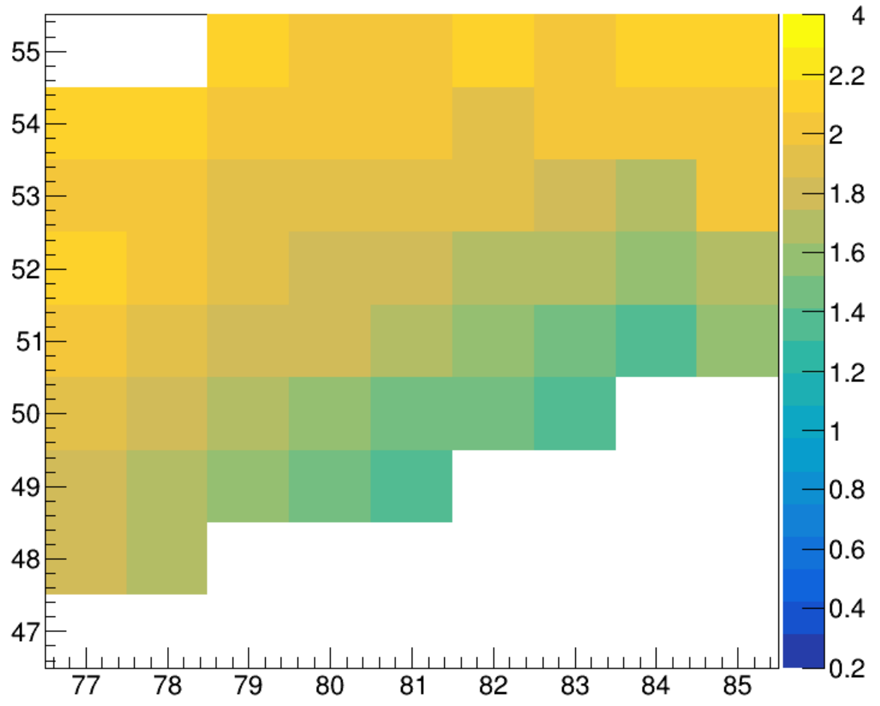

Mean FOLD, EXP

^{120}Cd example FF discrete gamma and FOLD equivalance

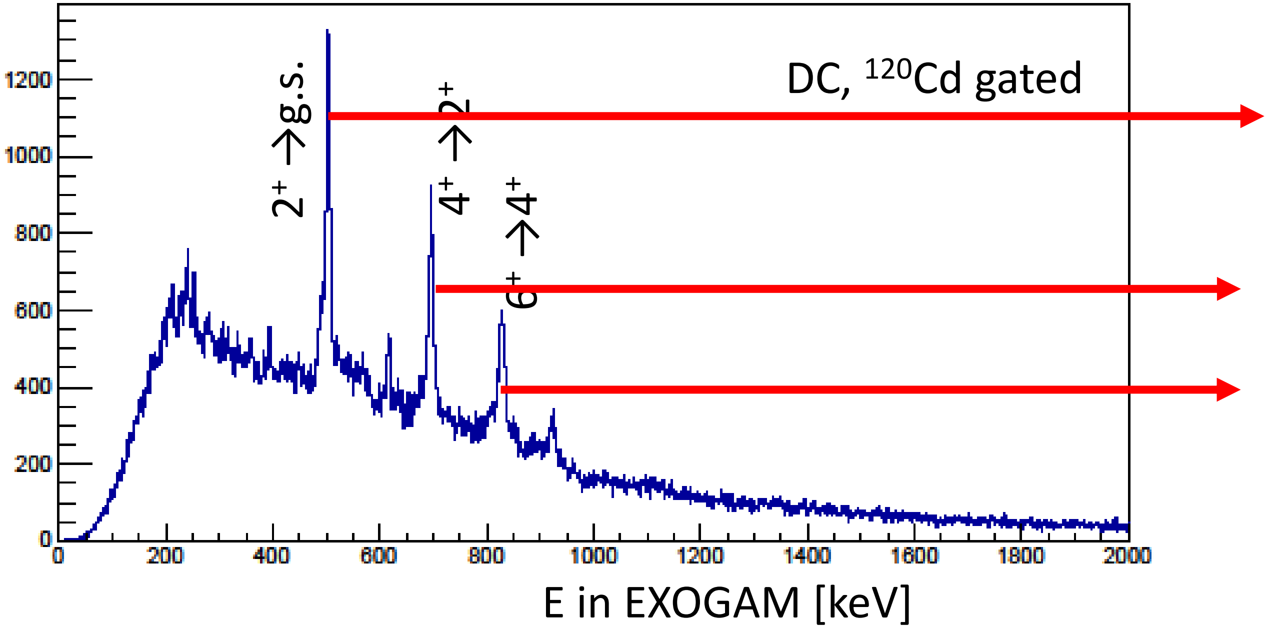

FF120Cd gated $\langle FOLD_{PARIS} \rangle = 2.66(1)$

FF120Cd &&FF_1 L≥2 $\langle FOLD_{PARIS} \rangle = 2.94(1)$

FF120Cd &&FF_1 L≥4 $\langle FOLD_{PARIS} \rangle = 3.07(1)$

FF120Cd &&FF_1 L≥6 $\langle FOLD_{PARIS} \rangle = 3.31(1)$

FIFRELIN code calculations, PFGS

EXP CALC

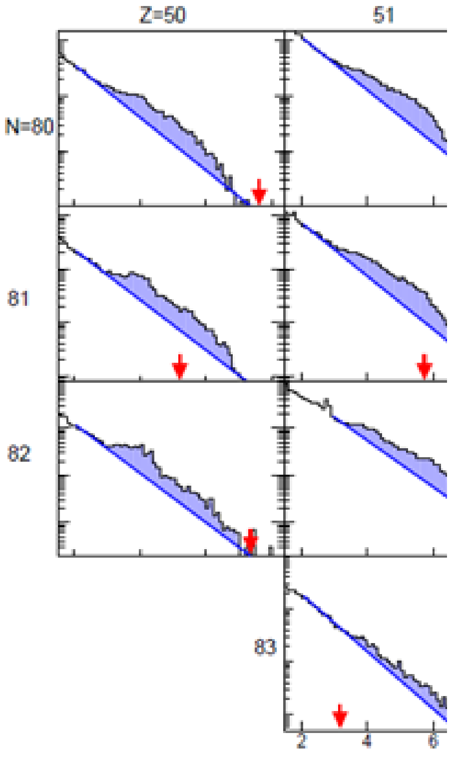

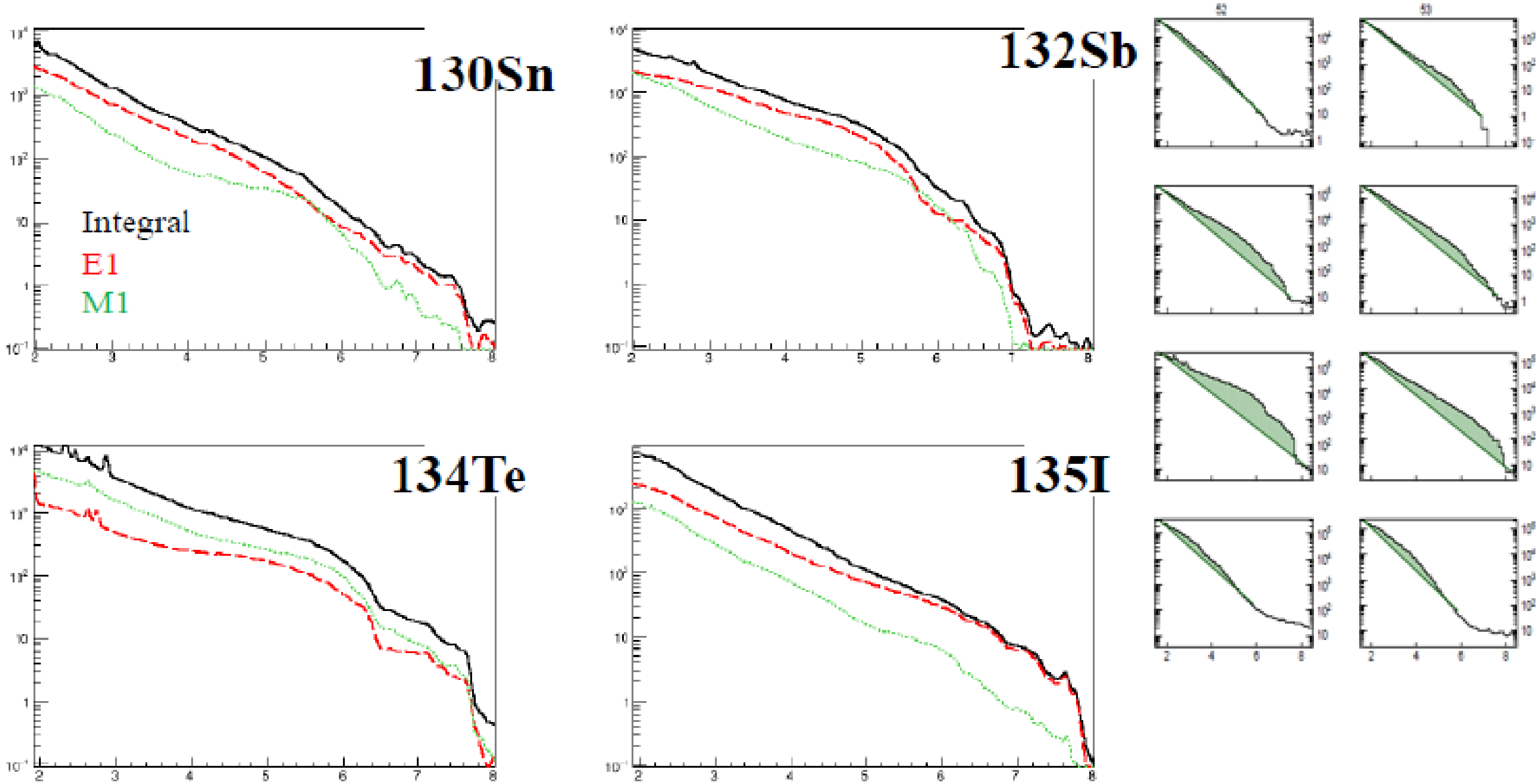

Sumary

Unique dataset for the PFGS (and PFNS) together with isotopically identified fission fragments was collected during experiment at GANIL with use of coupled VAMOS++ and PARIS+EXOGAM.

Scanning of the "gamma-bump" for entire fission fragment production and identification of its emitters in **Z and N** in the model-independent way was achieved for the first time.

Its existence was predominantly attributed to the proton composition of the fragment near the **Z = 50** shell closure, whereas its characteristics were influenced by the proximity to the **N = 82** neutron shell.

For entry point for the nuclei is at lower L around Z = 50 and N = 82, we see high energy structures in the gamma-ray spectrum which may be interpret as PDR (?) gamma-ray decay E1 type (or M1). **If it is true, then fission process can be another probe to investigate hard to reach neutron rich nuclides (otherwise accessible with huge difficulties with radioactive beams).**

Acknowledgements

Christelle Schmitt, M.C., Neeraj Kumar,

Piotr Bednarczyk, Sergio Brambilla, Manuel Caamano, Stefana Calinescu, Abdelhazize Chebboubi, Emmanuel Clement, Dominique Curien, Olivier Dorvaux, Gilles De France, François Didierjean, Gilbert Duchêne, Alain Goasduff, Iulia Harca, Yung Hee Kim, Grégoire Kessedjian, Maria Kmiecik, Antoine Lemasson, Silvia Leoni, Marek Lewitowicz, Olivier Litaize, Adam Maj, Iolanda Matea, Katarzyna Mazurek, Alahari Navin, Andreas Oberstedt, Stephan Oberstedt, Piot Julien, Diego Ramos, Maurycy Rejmund, Mihail Stanoiu, Louise Stuttge

and VAMOS, PARIS, EXOGAM collaborations

FIFRELIN, calc compositions